ELSEVIER

Medical Engineering & Physics 25 (2003) 239–253

Medical Engineering & Physics

www.elsevier.com/locate/medengphy

An implantable device for stimulation of denervated muscles in rats

Robert G. Dennis [a,b,c,d,*], Douglas E. Dow [b,c,d], John A. Faulkner [b,c,d]

[a] *Department of Mechanical Engineering, University of Michigan, Ann Arbor, MI 48109-2125, USA*
[b] *Department of Biomedical Engineering, University of Michigan, Ann Arbor, MI 48109-2007, USA*
[c] *Muscle Mechanics Laboratory, University of Michigan, Ann Arbor, MI 48109-2007, USA*
[d] *Institute of Gerontology, University of Michigan, Ann Arbor, MI 48109-2007, USA*

Received 19 February 2002; received in revised form 24 September 2002; accepted 15 October 2002

Abstract

The purposes of the present study were (1) to develop an implantable device capable of being pre-programmed to generate a protocol of chronic contractions in denervated hind-limb muscles of rats, and (2) to verify the design by implanting the stimulators for five weeks in rats to identify a protocol of stimulation that maintains muscle mass and maximum force in stimulated–denervated extensor digitorum longus (EDL) muscles. This implantable stimulator system did not hinder animal movement or hygiene, and enabled the animals to be housed in regular animal facilities, since neither external equipment nor an externally generated magnetic field was required. The pre-programmable microcontroller allows detailed basic research into the cellular and tissue response to different stimulation protocols. The micropower design of the battery powered device enabled chronic stimulation of denervated EDL muscles for the five weeks of this initial study. Stimulation protocols of 9–11 V pulse amplitude, 0.4 ms bipolar pulse width, 100 Hz, 20 pulses per contraction, and 100 or 300 contractions generated per day maintained muscle mass and maximum force in denervated EDL muscles of rats at values near control values for innervated muscles.

Keywords: Prosthesis; Contractility; Maximum force; Extensor digitorum longus; EDL; Programmable; Amplitude; Pulse; Bipolar; Micropower; Microcontroller; Tetanic contraction

1. Introduction

Electrical stimulation has long been employed to minimize the progressive atrophy and weakness that occur in denervated muscles [1–12], yet therapeutic electrical stimulation of denervated muscles has not become widespread clinically due to the lack of accepted standards and questions of efficacy [2]. Animal experiments can be employed to test a wide range of stimulation protocols, to identify effective interventions, and to study the basic biological mechanisms of the cellular and tissue response to various protocols. Animal studies in parallel with clinical studies [10–12] enhance overall understanding of the effect of electrical stimulation on denervated skeletal muscle. Devices for providing electrical stimulation of denervated muscle in human clinical studies have been described [10,13]. In this paper we describe the design for an implantable stimulator that is small, inexpensive, easily built, programmable and disposable, and is therefore suitable for use in non-clinical basic research, including implantation into small animals [14,15] and for use with tissue engineered skeletal muscle in culture [16–18]. The functional usefulness of this device was tested in two initial studies that compared protocols having different values for stimulation variables with the resulting outcome of muscle mass and maximum force.

The system we describe addresses several of the technical limitations that have arisen with earlier systems when employed in chronic studies with freely-moving small animals. The external wires and components of stimulation systems using surface electrodes [1,3,13,19–21], transcutaneous needle electrodes [4], and transcu-

* Corresponding author. Tel.: +1-734-936-2166; fax: +1-734-936-2116.
E-mail address: bobden@umich.edu (R.G. Dennis).

1350-4533/03/$30.00 © 2002 IPEM. Published by Elsevier Science Ltd. All rights reserved.
doi: 10.1016/S1350-4533(02)00193-5

taneous wires to implanted electrodes [5,6,22,23] are susceptible to damage, hinder animal hygiene and mobility, and increase the chance of infection. Systems that use an inductive link to power and control implanted circuitry and electrodes avoid these problems only if the coil that generates the magnetic field is outside the living space of the animal [24–26]. Such large coils require extra space and generate magnetic fields that would interfere with the fields of other nearby coils, making these systems incompatible with regular animal facilities.

Battery powered implantable stimulation systems are entirely internal to the body of the host. Therefore, animal hygiene and movement are not restricted, and the risk of damage or infection is reduced [27]. Each animal can be housed in regular animal facilities. Implantable stimulators have been used to generate contractions in innervated muscles [14], and non-programmable stimulators in denervated muscles of animals [15]. A partially programmable stimulator has been developed for denervated muscles of animals [9], but this stimulator design does not allow programmable modification of pulse width, length of pulse train, or irregular periods of rest between contractions that would enable protocols to have periods of more intensive work separated by variable periods of rest throughout a 24-hour day [9,10]. Stimulator designs based on programmable microcontrollers [28] have been shown to provide more flexibility for generating different protocols than devices based on state machines [14,15,28]. Programmability enables implanted stimulators to generate customized, complex protocols for experiments that optimize stimulation for desired contractile properties or cellular responses, such as targeted gene or protein expression. This level of flexibility is essential since no single stimulation protocol is "optimal" for all applications. The tissue response to a stimulation protocol differs depending on species [23] and fiber type composition [29].

The extensor digitorum longus (EDL) muscle of rats rapidly atrophies and weakens after the onset of denervation, and has been the subject of many studies of denervation [30–32] and of stimulation of denervated muscles [6,7,29,33]. Table 1 summarizes this research by corresponding the values of stimulation variables and the resulting muscle mass and maximum force. Electrical stimulation for 3 to 17 weeks of denervation has maintained muscle mass at 51 to 100 percent and maximum force at 6 to 70 percent of control values for innervated muscles. No reported stimulation protocol has maintained both mass and force at control values.

The purposes of the present study were (1) to develop an implantable device capable of being pre-programmed to generate a protocol of chronic contractions in denervated hind-limb muscles of rats, and (2) to verify the design by implanting the stimulators for five weeks in rats to identify a protocol of stimulation that maintains muscle mass and maximum force in stimulated–denervated extensor digitorum longus (EDL) muscles. We desired to design a stimulator that would be economical and readily assembled to enable a broad spectrum of researchers to utilize (and customize) this stimulator design for investigations into the functional and cellular response of denervated muscles to different protocols of stimulation. Our initial animal experiments verify the functionality of the stimulator system, and test the hypotheses that (1) contractile activity generated by an electrical stimulator can maintain muscle mass and maximum force at values similar to control values of innervated muscles and (2) contractions sufficient to maintain muscle mass and maximum force are not generated if the number of pulses per contraction or the pulse amplitude is too low.

2. Methods: detailed stimulator design, assembly and testing

2.1. Stimulator system design

The circuit design is diagrammed in Fig. 1 and corresponding components are listed in Table 2. The hardware functions correspond to I/O pins on the microcontroller. The microcontroller pins are numbered beginning with #1 (upper right corner in Fig. 1), and continuing counterclockwise around the 20-pin microcontroller. The output transistors are controlled by pins 1, 2, 19 and 20. Power (+2.8 to 3.0 V) is supplied to pins 3, 4, 15, and 16. Pins 5 and 6 are connected to ground. The magnetic reed switch connected to pin 14 allows simple communication with an externally generated magnetic field while the device is implanted. This was used to begin or end SLEEP mode of the stimulator, and to generate a test train of pulses for one muscle contraction. The phototransistor and LED are optional components that allow transcutaneous bi-directional serial communication between the implanted device and an external optical interface. For the stimulators built for the animal experiments described below, optical communication was not used.

Many design choices were driven by the effort to minimize power consumption. Micropower design is essential for any implantable device. Stimulation of muscles that have been chronically denervated requires many times the energy required for either nerve stimulation or direct stimulation of acutely denervated muscles. The number of batteries to supply power is limited, since the total mass of the device ideally should not exceed 5% of the body mass of the animal [15]. To save power the supply voltage was set at a low value of ~2.8 V since current drain and power consumption rise as supply voltage rises as plotted in Fig. 2. The device needed to be designed to operate properly over the range of 2.70 to 3.15 V, because the lithium battery power source was

Table 1
Published results of electrical stimulation systems to maintain mass and maximum force in denervated–stimulated rat muscles. All cases were stimulated 24 hours per day using subcutaneous electrodes, and either bipolar or alternating polarity pulses. Column heading descriptions follow. F_p is the frequency of stimulation pulses that generate each contraction. P_c is the number of pulses to generate one contraction. The time duration of one bipolar pulse is t_p. C_d is the number of contractions generated each day, usually separated by periods of rest having equal durations. A is the amplitude of each stimulus pulse, and is the electric current (mA) that flowed between the electrodes during each pulse. Weeks Denrv–Stim is the number of weeks that the EDL muscle was simultaneously stimulated and denervated. Mass % Cntrl is the muscle mass as a percent of mass of innervated control muscle, and Force % Cntrl is the maximum force that the muscle could generate during an isometric tetanic contraction, as a percent of force of innervated control muscle

F_p (Hz)	P_c	t_p (ms)	C_d	A (mA)	Weeks Denrv-Stim	Mass % Cntrl	Force % Cntrl	Reference
150	46	0.4	1440	5–10	3–10	82	70	[7]
150	25	0.4	5760	5–10	5–12	108	69	[6]
100–200	3	0.4	864	5–10	3–12	84	59	[6]
150	25	0.4	96	5–10	5–12	85	57	[6]
20	7	0.4	1440	5–10	3–10	56	29	[7]
20	200	0.4	2880	5–10	5–12	64	27	[6]
100	60	0.2	1440	5–10	8–17	51	6	[41]

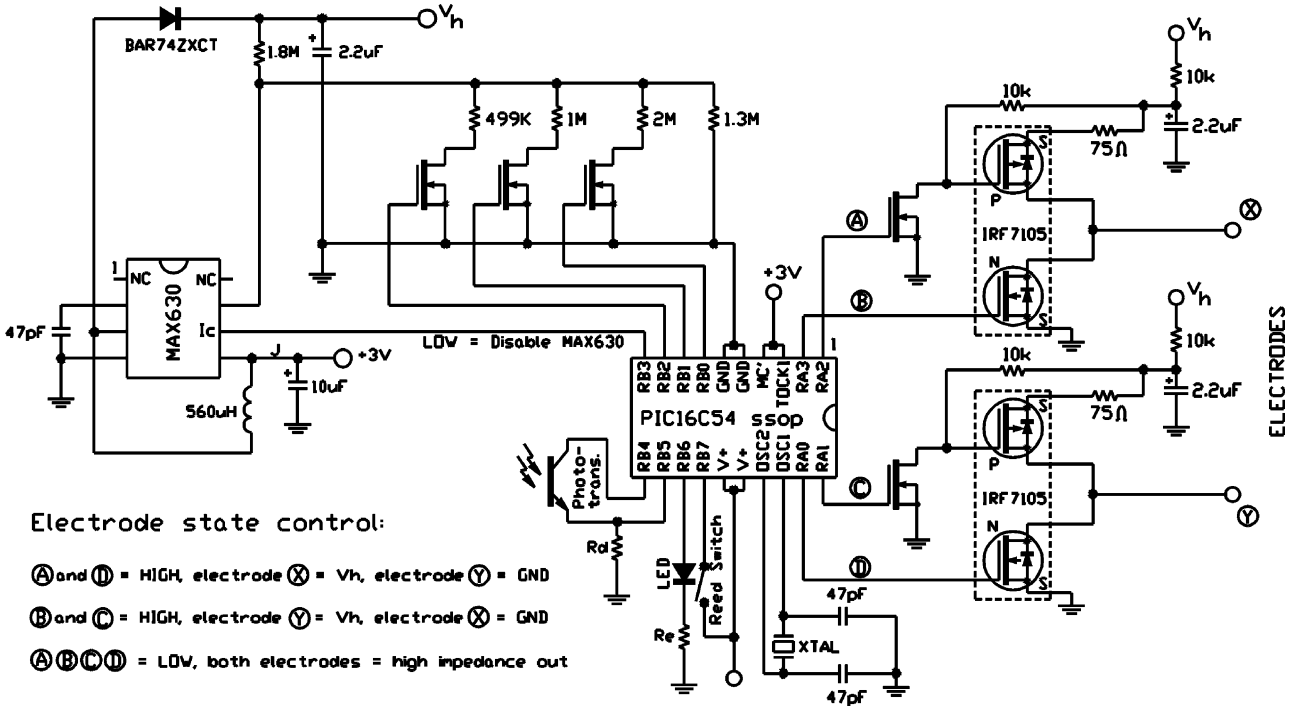

Fig. 1. Schematic for stimulator for use with denervated muscle. The DC—DC converter (MAX630) permits high voltage stimulation with only a single 3 volt battery. Output voltage is controlled by software. A magnetic reed switch allows the user to control the operating mode of the stimulator even after implanted. HEXFET buffers allow tri-state outputs (high-impedance, ground, and V_h). Components used are listed in Table 2.

unregulated, and the voltage discharge curve for nominally "3 volt" lithium batteries spans this range [15], though the longest operational plateau is ~2.80 V.

The PIC16C54A-04 microcontroller was selected because it uses less power than other functionally identical microcontrollers, especially the PIC16C54C-04 (Fig. 2). Lithium batteries supplied the circuit in our final design at ~2.8 V. Unlike many other stimulation systems [5,6,22,23], we employed voltage control of the stimulus pulse amplitude rather than current control. This simplified the stimulator architecture and improved micropower performance.

A general principle of micropower design is to use the largest values of resistors and the smallest values of capacitors as possible to minimize power consumption. Any unused I/O pins of the microcontroller were set to INPUT mode during initialization of the software, and the pins were pulled to ground in hardware using 1 MΩ resistors. Energy is lost each time a capacitor is cycled from the charged to the uncharged state. The 2.2 μF discharge capacitors are necessarily large, but not excessively so. The inductor for the MAX630 DC–DC converter was set at 560 μH, even though that was three orders of magnitude below the specifications of the

Table 2
List of components for the circuit in Fig. 1

DigiKey catalog #	Value and description
P220KABK-ND	220.0 kΩ (0805 SMD)
P2.0MGCT-ND	2.0 MΩ (0603 SMD)
P10.0KHCT-ND	10.0 kΩ (0603 SMD)
P10.0KLCT-ND	10.0 kΩ (0402 SMD)
P1.0MGCT	1.0 MΩ (0603 SMD)
P75ACT-ND	75 Ω (0805 SMD)
P2045-ND	2.2 μF Capacitor
PCC470ACVCT-ND	47.0 pF Capacitor (0603 SMD)
PCT3106CT-ND	10.0 μF Capacitor
BAR74ZXCT-ND	Diode
ZVN3306FCT-ND	MOSFET Transistor
DN1145CT-ND	560 μH Inductor
HE500-ND	Magnetic Reed Switch
SE3316-ND	40 kHz Crystal Oscillator
MAX630CSA-ND	IC Chip, DC-DC Voltage Converter
IRF7105-ND	IC Chip, F7105, HEXFET transistors
PIC16C54A-04/SS-ND	8-bit Microcontroller, Microchip
P199-ND	Battery, 3V, 255 mAh, Lithium Coin with legs

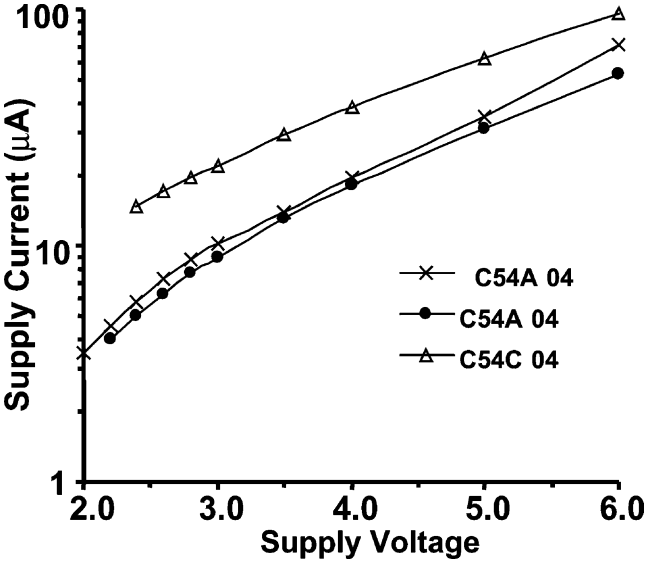

Fig. 2. Supply current as a function of supply voltage. Baseline operating current for each type of microprocessor, with a 40 kHz clock, is measured. Current drain depends upon the specific microprocessor type: PIC16C54C-04 (△), PIC16LC54A-04 (×), PIC16C54A-04 (●). Though these devices are functionally the same, one consumes much more power than the others. Selection of the specific microprocessor was made on the basis of minimum operating current.

manufacturer for the MAX630. The smaller inductor consumed less power and space than the recommended one.

The selection of this inductor value depended upon both the maximum desired voltage and the current drain of the device. For this application of stimulating denervated muscles, the required duty cycle of the stimulus pulses is relatively low, making the total energy transfer through the DC–DC converter low. The very fast switching diode (BAR74ZXCT) was selected to minimize the loss of energy through transient "backflow". The microcontroller software configuration was set to operate in Low Power crystal oscillator mode, and the Watch Dog Timer was disabled, as it would draw considerable current to operate the independent internal RC oscillator circuit. The crystal oscillator frequency was selected to be close to the lowest possible speed to minimize power consumption since current drawn by the microcontroller increases linearly with clock speed. We employed a 40 kHz oscillator crystal, which results in an instruction cycle time of 0.1 ms, sufficiently fast to program the 0.4 ms bipolar pulse width required by our stimulation protocol.

The stimulator provides source current for stimulation pulses that have sufficient amplitude to generate contractions in the target denervated muscle. The ideal amplitude would be just high enough to ensure that each muscle fiber depolarizes and contracts, but not to cause tissue damage from excessive current density. The required amplitude of the pulse to depolarize each muscle fiber is directly affected by the level of excitability of the denervated muscle fibers , muscle size and architecture, and electrode placement.

Fig. 3 shows results of a preliminary study that helped determine the range of output voltages and current flow that would be necessary for generating contractions in stimulated–denervated EDL muscles of rats. EDL muscles of rats were denervated by transection of the sciatic nerve high in the thigh region [30,35] with and without stimulation for 10 days. The current flow between the two stimulation electrodes that looped around the belly of the muscle (Fig. 4) and the resulting muscle force for a range of pulse voltages was measured with the rat in an in situ preparation using a shoe apparatus [36]. The stimulation pattern during these measurements consisted of unipolar pulses having 0.2 ms pulse width, 150 Hz, and 15 pulses per contraction. This in situ preparation did not isolate contractile activity of only the EDL muscle, the adjacent muscles may also have been recruited and generated force. Nevertheless, the setup did demonstrate the lower voltage threshold necessary to generate any contractile force. The higher voltages were expected to recruit more and more adjacent muscle fibers and not just the EDL muscle fibers that the electrode wires looped around. Fig 3(A) shows that a stimulator should generate pulses having amplitude in the range from 4 V to above 12 V. Fig 3(B) shows that the stimulator must be able to source output current of at least 25 mA.

The design of the stimulator provides flexible setting of the pulse amplitude, since the amplitude may have to be adjusted for optimal effect in each application. In Fig. 1, pins 7, 8, and 9 control the stimulation voltage by setting the reference voltage on the MAX630 DC–DC

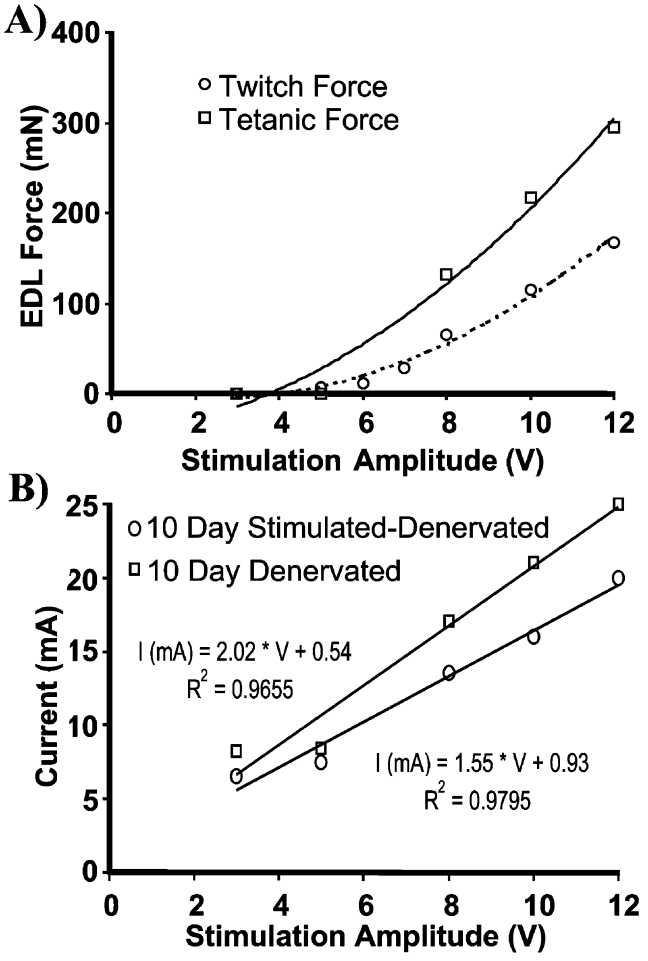

Fig. 3. Preliminary data was used to determine the range of pulse amplitudes that generate EDL muscle contractions and to determine equivalent resistance of EDL muscles of rats. Force (A) and current flow (B) are plotted as functions of stimulation pulse voltage. EDL muscles of rats were denervated with or without stimulation for 10 days prior to these measurements, which were made in an in situ preparation using a shoe apparatus [36]. The stimulation pulses were passed to the EDL muscle through loop electrodes similar to the ones pictured in Fig. 4. The stimulation pattern during these measurements consisted of unipolar pulses having 0.2 ms pulse width, 150 Hz, and 15 pulses per contraction. (A) Force generated by EDL muscles are plotted against the amplitude of the pulses. Torque values were measured in situ at the ankle and corresponding force values for the EDL muscle were calculated by the method of Miller and Dennis [36]. The circles and dashed line show the generated force values for twitch contractions, and the squares and solid line show force for tetanic contractions. Lines are the best-fit 2nd order polynomial fit to the data. With increasing voltage, other muscles near the EDL may be recruited, adding to the force level. Control values for normally innervated rat EDL muscles are generally greater than 2000 mN. (B) The equivalent resistive load for this electrode configuration is shown for both denervated and denervated–stimulated muscles. The slope of the best-fit linear regression indicates the equivalent resistance for loop electrodes, which is ~500 Ω for 10-day denervated muscle, and ~650 Ω for denervated–stimulated EDL muscle.

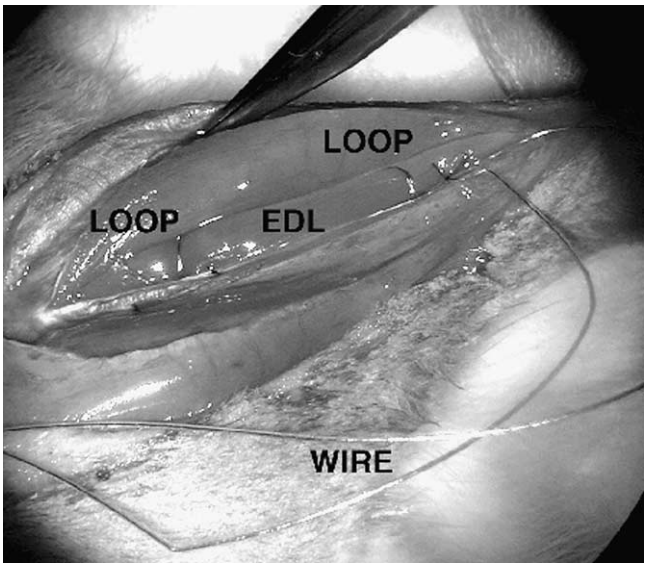

Fig. 4. Surgical placement of the loop electrodes. The stainless wire electrodes (Cooner Wire # AS633, 36 AWG stranded stainless steel) were looped around the proximal and distal ends of the EDL muscle as shown, and at least 10 mm separated the two loops. The Teflon wire insulation was removed from the ends of each electrode wire by mechanical stripping using a sharp-edged hard plastic object, such as a plastic butter knife, to avoid nicking the steel wire. The insulation was stripped away far enough to allow a loop of exposed wire to be formed around each end of the muscle. The ends of each electrode wire were spiraled away from the mid-section of the muscle, toward the closest tendon.

converter. Pin 10 controls the DC–DC converter mode (enable/disable). During periods between muscle contractions when the DC–DC converter is not required, it is disabled to minimize power consumption. The voltage converter generates a voltage level (V_h), which corresponds to the pulse amplitude. The voltage converter is tuned by a voltage divider connected to pin 7 of the MAX630 chip (Fig. 1). The output of the voltage divider is set by software (to select which lower resistors are active) and hardware (values of the lower resistors). The high side resistor (R_H) of the voltage divider was set at 1.8 MΩ. On Fig. 1, R_H is the "1.8 M" resistor connecting pin 7 of the MAX630 to the stimulation voltage V_h. The low side resistor (R_L) value is the Thevenin equivalent parallel resistance of the combination of the other four resistors connected to pin 7 of the MAX630. Three FETs allow R_L to be adjusted by determining which resistors are included in the parallel Thevenin equivalent resistance. The FETs are switched ON or OFF by embedded software that controls the logic state of RB0, RB1, and RB2 of the microcontroller. This determines the value of R_L, which in turn controls the DC–DC converter output voltage. With three FETs, each paired with a resistor, 8 possible voltage levels can be defined. Given a desired stimulation voltage level (V_h) for the DC–DC voltage converter, the required value of the lower resistors (R_L) was calculated as follows:

$$R_L = 2385/(V_h - 1.325) \quad (1)$$

where R_L is measured in kΩ and V is in volts. The form of the equation was derived from the MAX630 data sheets and the constants were determined experimentally. The supply currents required for various output voltages are plotted in Fig. 5. The relation between the equivalent value of R_L and the resulting output voltage generated by the DC–DC voltage converter and the required supply current for each value of R_L are plotted in Fig. 5(A). Fig 5(B) shows that higher levels of voltage generated by the DC–DC voltage converter result in higher current drain, even when no load was placed across the output electrodes.

The stimulator circuit consumes different amounts of current depending on whether the DC–DC converter is enabled or disabled. Fig 6 plots this relationship, showing that more supply current is required when the voltage converter is enabled than when it is disabled. The plot

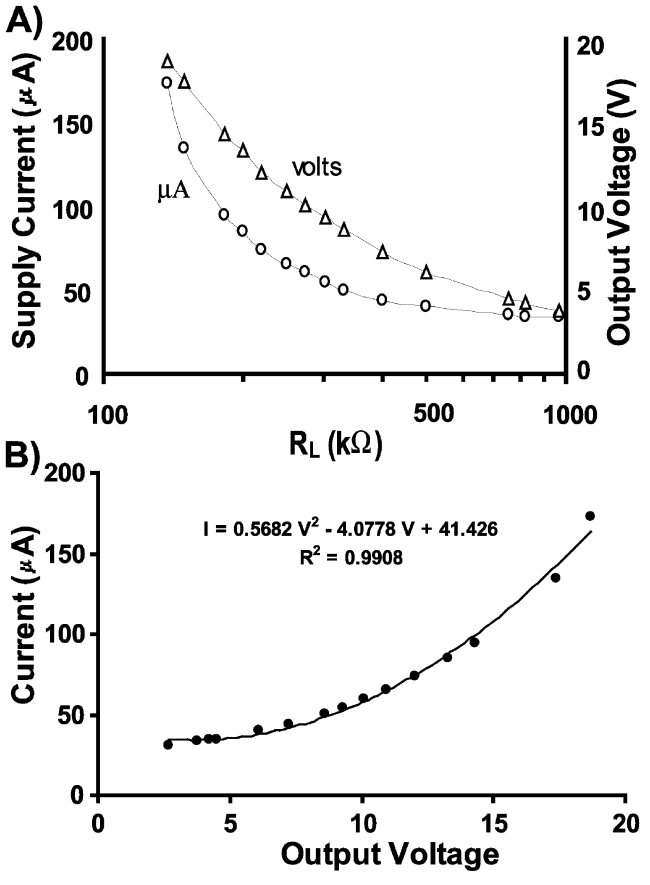

Fig. 5. Control, current drain, and output voltage (V_h) of the DC–DC voltage converter. V_h can range from the battery supply voltage (~2.80 V) up to ~18 V and the generated level is tuned by a voltage divider circuit (Fig. 1) between R_H and the equivalent value of R_L. The stimulator was operated at ~2.8 V, a 560 μH inductor coil was used, and there was no load between the output electrodes. (A) The equivalent low-side resistor (R_L) tunes the DC–DC voltage converter. The lower the value of R_L, the higher the output voltage (V_h), and the higher the current drain and power consumption. (B) The higher the output voltage (V_h), the higher the current drain and power consumption.

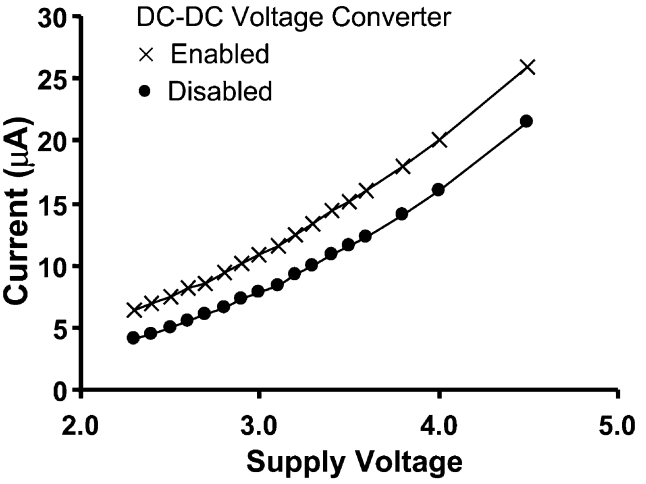

Fig. 6. Supply current of the stimulator circuit as a function of supply voltage for when the DC–DC voltage converter is either enabled or disabled. The higher the supply voltage, the more the current drain and power consumption. The solid dots (●) are when the DC–DC converter was disabled, and the crosses (×) are when the DC–DC converter was enabled and set at V_h=9 V. The outputs had no resistive load during these measurements.

also affirms that more supply current is consumed as the supply voltage increases. At the supply voltage of 2.8 V for the stimulator, the required supply current increased from about ~6 to ~9 μA when the DC–DC converter was enabled. Therefore, to maximize battery life the software was programmed to disable the voltage converter during the periods of rest between the trains of pulses.

A flow chart for the software of the stimulator program is in Fig. 7. Software was written in C and cross-compiled (Custom Computer Services Inc., Brookfield, WI). Upon power-up, the program of the microcontroller configures the I/O pins, disables the DC–DC voltage converter, and enters SLEEP mode to save power. Thereafter, upon detection of an external magnetic field that closes the reed switch, the microcontroller exits SLEEP mode, resets internal counters, and proceeds to run the stimulation protocol. The software interprets closure of the magnetic reed switch in a context-sensitive manner to control multiple functions: (1) set the stimulator into and out of SLEEP mode, and (2) elicit a test contraction. The software program conserved power by enabling the DC–DC voltage converter only during the generation of a train of pulses to generate one muscle contraction (Fig. 6). In the tested stimulation protocols, the train of pulses for one contraction was much shorter in duration than the period of rest between contractions, so disabling the converter between contractions conserved power.

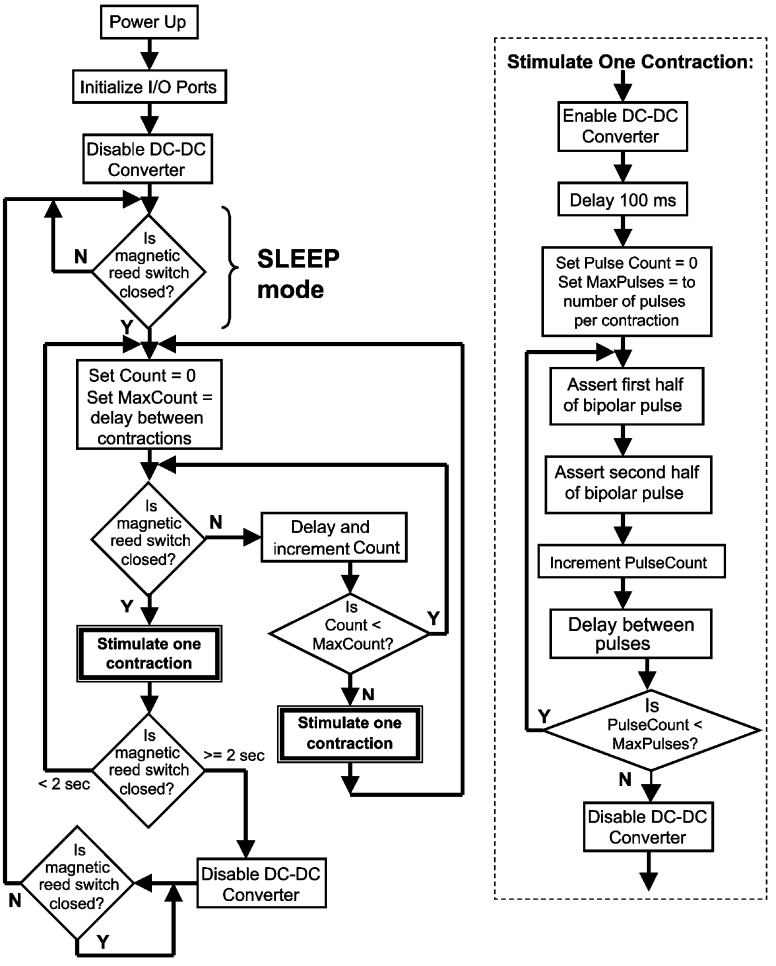

Fig. 7. Program flow for the implantable stimulator used in this series of experiments. At power up, the program initializes and enters SLEEP mode where the output remains in a high impedance mode until an external magnetic field closes a reed switch. At this point the system begins the stimulation protocol, generating one muscle contraction separated by determined periods of rest where the output remains in a high impedance mode. At any time, if the external magnetic field closes the reed switch for longer than 2 seconds, the program enters SLEEP mode.

2.2. Stimulation protocols

The stimulator was programmed to generate symmetrical and balanced bipolar pulses as diagrammed in Fig. 8. Unipolar pulses or unbalanced bipolar pulses result in net ion flow, tissue damage, and corrosion of the anode electrode surface [37–39]. The stimulator design generates balanced and symmetrical pulses to minimize net ion flow. In preliminary trials, we inspected the electrode surfaces after implantation and a period of stimulation–denervation, and found that the electrode surfaces for unipolar or non-symmetrical bipolar pulses showed clear evidence of corrosion of one or both electrodes, whereas the electrode surfaces for the balanced, symmetric bipolar pulses that were either paired (Fig. 8(A)) or alternating (Fig. 8(B)) showed no sign of corrosion on either electrode. To further protect the tissue and electrodes from hydrolytic damage and corrosion, we utilized high impedance outputs during the time intervals between stimulus pulses to eliminate current flow between the electrodes that might arise from ground state imbalance or leakage. This had the further advantage that the physiologically normal voltage gradient within the tissue could be restored between contractions.

The rationale for the values of the stimulation variables that were programmed into the stimulators used in the animal experiments of this study is as follows. As seen in Fig. 8, the pulse width (t_p) of the paired bipolar pulses is the total time duration of both halves of the stimulation pulse, and t_p was set in the program to be 0.4 ms, based upon our preliminary data and previously published reports [6,7,34]. As diagramed in Fig. 9(A), F_p is the frequency of pulses during a train of pulses that are to generate one muscle contraction, and was programmed to be 100 Hz. The stimulators were programmed to generate either 100 or 300 contractions per day (C_d), each separated by equal intervals of rest.

The parameters to be varied in these experiments were pulse amplitude (V_p, diagrammed in Fig. 8) and pulses per contraction (P_c, diagrammed in Fig. 9(B)). The

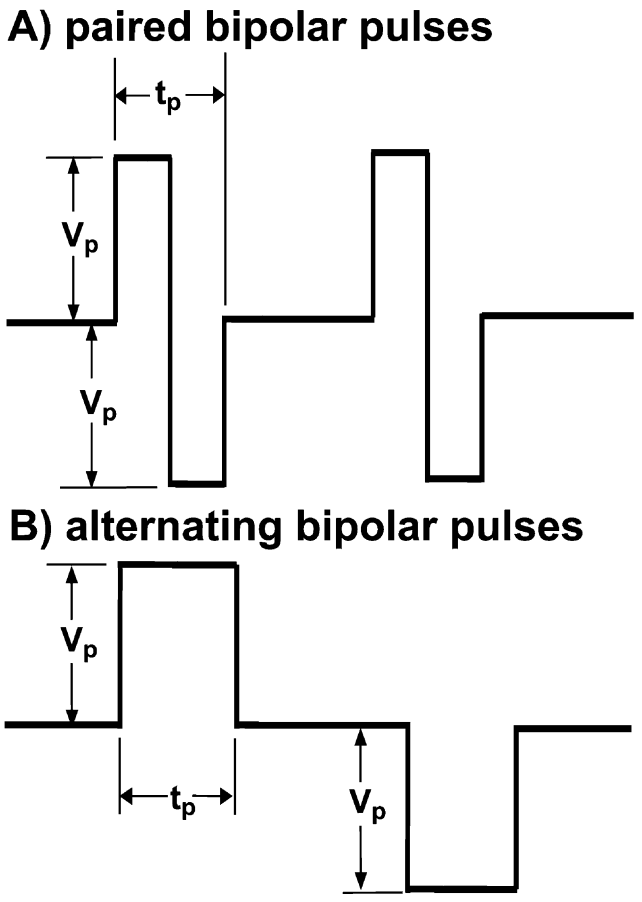

Fig. 8. The microprocessor software determines the form of the bipolar pulses. Paired bipolar pulses (A) were used in this study to balance charge and prevent a net ion flow between the electrodes, which would cause a toxic reaction in the tissue. The net current flow was balanced with bipolar pulses in which the positive and negative half-pulses have equal voltage amplitudes and pulse widths. Alternating bipolar pulses (B) would also have balanced net current flow, but were not tested in the animal experiments reported here. Pulse width (t_p) is the total time duration of each bipolar pulse. Voltage (V_p) is pulse amplitude, positive and negative from resting voltage levels.

values of V_p to test in this experiment (0, 5, 7, 9, and 11 V) were selected on the basis of a preliminary experiment that determined the pulse amplitude necessary to elicit sub-maximal contractions of the EDL muscle of rats using implanted loop electrodes as plotted in Fig. 3(A). The values of P_c to test were 0, 3, 6, and 20 pulses per contraction, and were selected based on preliminary data and the results of Eken and Gundersen [6]. Each stimulated–denervated EDL muscle received a protocol of stimulation for 24 hours per day for the duration of five weeks between the onset of denervation until the final evaluation of the muscle.

Beyond the ranges of values for the stimulation parameters that we utilized, the design allows the stimulator to be programmed to generate other protocols. For instance, the pulses generating one contraction do not have to be generated at a single frequency. Different contractions could be generated by pulses having different amplitudes. The interval between contractions does not have to be fixed, such that layered periods of more and less intense work could be separated by periods of rest throughout a 24-hour period.

The energy utilization of this device depends predominantly on the stimulation protocol. As a rule of thumb, all of the active stimulation parameters, such as t_p, F_p, P_c, and C_d should be set to the minimum possible values that will yield satisfactory physiological results in order to prolong the functional duration.

2.3. Assembly and testing

The stimulators were assembled, pre-tested, and encapsulated as follows. The printed circuit boards (PCBs) were made using prototype printed circuit etching methods [15], or were designed and ordered through an on-line PCB production service (expressPCB.com). The electrical components of the circuit were soldered into place on the PCB. After assembly, each stimulator was powered by an external voltage supply set to 2.80 V. With the stimulator set in SLEEP mode and the electrodes not connected to a load, the current draw was measured using a digital ammeter. Circuits with current drain above 10.0 μA (Fig. 2) were inspected and repaired, or else discarded. Function was verified by sweeping a magnet near the reed switch on the stimulator to generate a test train of pulses and observing the generated voltage waveform between the two output connections using a differential input digital oscilloscope to measure and verify correct values for pulse amplitude (V_p), pulse width (t_p), frequency (F_p), and number of pulses per contraction (C_d). Teflon coated, multi-stranded, stainless steel electrode wire (36 AWG; AS633, Cooner Wire, Chatsworth, CA) was cut to a length at least 30% longer than required to span the distance from the implantation site to the target tissue in order to minimize tension during animal movement. The stainless steel wire was soldered to the copper patches on the PCB as described earlier [15].

After passing initial tests, the circuits were connected to two lithium batteries (255 mAh capacity), which were determined to be sufficient for the duration of this experiment [15]. Lithium batteries were selected since they provide the best energy density among commonly available batteries that do not vent gases, which would be toxic to the tissue and incompatible in a tightly sealed implantation chamber. The batteries were connected in parallel to lithium batteries that maintained a voltage supply of ~2.8 V for the operational life of the device. Powering the circuit with voltage below 3.0 V minimizes "class A" current loss during switching in the microcontroller.

Each assembly was then encapsulated with a thin layer of electrical-grade epoxy (DP-270 clear Epoxy, 3M

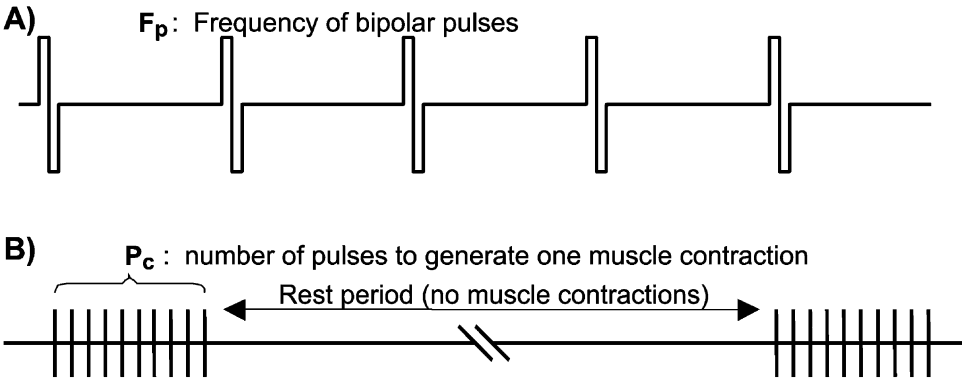

Fig. 9. Definition of the stimulation variables of frequency (F_p) and pulses per contraction (P_c). (A) Frequency (F_p) is the rate of bipolar pulses during each pulse train that is to generate one muscle contraction. F_p is measured in Hz. The pulse amplitude is maintained at ground state (0.00 V) between pulses within a pulse train. (B) Pulses per contraction (P_c) is the number of pulses at the given frequency (F_p) during one pulse train that is to generate one muscle contraction. Each muscle contraction is separated by periods of rest during which no electric pulse or voltage signal is asserted between the two electrodes that are in contact with the denervated–stimulated muscle. Between pulse trains, the output state of both electrodes is set to high impedance, not ground state.

Adhesives Division, St. Paul, MN) covering only the printed circuit board components. Small but loose knots were tied in the electrode wires at the exit point from the stimulator. The knots and circuit were encapsulated with a thinned one-part silicone adhesive [15]. The encapsulated knots allowed slack and minimized tension on the wires during and after surgical implantation. The outer dimensions of the final encapsulated device were ~5.5×2.5×1.0 cm, with a total mass of ~19 g. The mass was 5.4% of the mass of a 350 g rat, slightly above the design goal of ≤5% of the mass of the host [15].

After encapsulation, the function was verified again by sweeping a magnet near the stimulator and observing the voltage waveform between the two output wires using an oscilloscope. During this functional test a load of 1.6 kΩ was placed between the electrodes to simulate tissue impedance. A resistor load in the range between 0.5 kΩ to 3 kΩ would have been expected to adequately serve this purpose.

Many different versions of the software for the microcontroller were made throughout the development of this system and the generation of experimental data. To test and verify that each software version generated the correct stimulation protocol when actually running in the circuit, the program was compiled and loaded into a stimulator circuit, a 1.6 kΩ load was placed across the output electrodes, and the stimulator was powered and brought out of SLEEP mode. The stimulator output over a period of 24 hours was recorded by a PC running a LabVIEW (National Instruments, Austin, TX) program that we developed for this purpose. The parameters of the recorded waveform were compared with the desired stimulation variables to ensure correctness.

After functional testing, each encapsulated stimulator was given a non-destructive, heat-failure test in an agitated, isotonic, saline bath. The duration of the heat test was 24 hours and the temperature of the bath was held at 50°C to minimize degradation of the battery life prior to implantation. Afterwards, the devices were removed from the saline bath, rinsed in tap water, and functionally tested again using an oscilloscope. This test was designed to detect “infant mortality” of the stimulators that would arise from incomplete encapsulation, or other defects that would make the devices vulnerable to rapid failure in a saline environment. Any stimulators that became defective during the heat test were not implanted into rats. Devices that passed the test were encapsulated with one additional layer of silicone.

To anchor the stimulator and prevent subcutaneous migration after implantation, a patch of prolene mesh (Ethicon Inc., Somerville, NJ) of approximate size 25×25 mm was affixed to the final silicone encapsulant layer by drops of additional silicone adhesive. The stimulators were stored at room temperature in SLEEP mode with electrode ends carefully separated.

3. Methods: animal experiments

3.1. Surgical denervation and implantation of the stimulators

The experiments were carried out using specific-pathogen-free male rats of the Wistar/Hicks–Carlson strain (Harlan Sprague Dawley, Indianapolis, IN). All procedures were conducted in accordance with the guidelines established in the United States Public Health Service Guide for the Care of Laboratory Animals (NIH Publication 85-23) and with the approval of the University Committee on the Use and Care of Animals. For surgical procedures rats were anesthetized with an initial intraperitoneal injection of pentobarbital sodium (60 mg/kg) followed by supplementary doses to maintain a

deep plane of general anesthesia. All surgical procedures were performed using aseptic techniques.

Muscle denervation and implantation of the stimulators were performed during the same surgical procedure. EDL muscles in both the denervated and stimulated–denervated groups were denervated according to the "high-sciatic" procedure of Carlson and Faulkner [30,35]. Briefly, after the rat was anesthetized the sciatic nerve was exposed in the thigh region and tightly ligated in two places about 5 to 10 mm apart, and the nerve segment in-between was removed. The resulting nerve stumps were implanted into separate muscular tissue as far away from each other as possible. This method of denervation has been shown to reliably prevent autoreinnervation of the EDL muscles of rats for at least 22 months [35].

To minimize the risk of infection, the implantable stimulators were dipped in 70% ethanol prior to implantation, and implanted below the skin on the back of the rat. The electrode wires were tunneled subcutaneously from the stimulator to the EDL muscle in the right hindlimb using blunt dissection techniques. In the hind limb, the wires were sutured to adjacent muscles and connective tissue for mechanical stability. A length of loose electrode wire was lightly sutured into place near the target muscle in order to minimize mechanical loading of the electrode ends, which were looped around the muscle. The two wire loop electrodes used in this study were implanted as pictured in Fig. 4. Loop electrodes were constructed simply by removal of about 1.5 cm of insulation from the end of each electrode wire, leaving the stainless steel strands clean and exposed. The loops were positioned equal distances from the distal and proximal ends of the muscle, and were separated by at least 10 mm for the 30–36 mm long EDL muscle.

In preliminary experiments we found that loop electrodes (with a larger surface area) performed better than smaller "pin" electrodes that were made by stripping 2 or 3 mm of insulation off the ends of the wires and suturing those into the muscle. The pin electrodes resulted in significant tissue damage in the quadrant of the tissue cross-section between the electrodes. This tissue damage may have resulted from excessive current density for the smaller surface area of the interface between the electrode and the muscle tissue, though the pin electrodes did not exhibit visible corrosion after the weeks of stimulation–denervation.

The implanted stimulators remained in SLEEP mode for one day following implantation during which the denervated muscle received no electrical stimulation to generate muscle contractions. One day after implantation, a magnet was passed near the awake and freely moving rat adjacent to the location of the stimulator to momentarily close the magnetic reed switch and trigger the software (Fig. 7) to exit SLEEP mode and initiate the stimulation protocol. A train of stimulation pulses generated a muscle contraction resulting in visible toe and foot movement. The rats did not show signs of pain caused by the electrical stimulation in the denervated leg.

3.2. Muscle evaluation

For five weeks following denervation and implantation, the right EDL muscles either received no stimulation (denervated group) or were denervated and stimulated (stimulated–denervated groups) prior to in vitro evaluation of muscles harvested from anesthetized rats. The left EDL muscle served as an innervated control, receiving no surgical intervention or electrical stimulation (control group) prior to muscle evaluation. After the period of five weeks, the maximum force and muscle mass of each EDL muscle were determined. The rats were anesthetized during this procedure, and later euthanized with an overdose of anesthesia.

The muscles were evaluated in vitro according to the procedure of Carlson and Faulkner [30,40]. Briefly, the EDL muscles were exposed and dissected free of other tissues. Sutures were placed around the distal and proximal tendons, tendons severed, and the muscle placed into a bath of Krebs–Ringer bicarbonate solution maintained at 25±0.5°C and gassed with 95% oxygen and 5% carbon dioxide. One tendon was tied to a fixed post and the other to a force transducer. Muscles were electrically stimulated by square, unipolar pulses (t_p=0.2 ms) generated between platinum plates separated by 20 mm placed parallel to the muscle, one electrode plate on either side of the muscle in the bath. The voltage was adjusted slightly greater than that necessary to produce a maximum isometric twitch contraction. The muscle length was adjusted to optimum length for force development. The maximum force (maximum isometric tetanic force) was determined by increasing the frequency of stimulation until the force reached a plateau. The muscles were then removed from the bath, tendons trimmed, and weighed. The muscles were frozen by immersion in a mixture of dry ice and isopentane, and later were sectioned at 10 μm through the middle portion of the muscle. The sections were stained with hematoxylin and eosin for viewing under a light microscope.

4. Results: animal experiments

4.1. Functionality of the implanted stimulator

Once implanted, the size and mass of the stimulator seemed to be well tolerated by the rats. Connective tissue was found to have bonded to the prolene mesh that was affixed to the stimulator, minimizing subcutaneous migration. The two lithium batteries (255 mAh) were found to be sufficient to power the stimulators for all of

the tested protocols of stimulation, such that visible foot and toe movement could be visually seen during test contractions throughout the duration of five weeks of stimulation. Each stimulator that was implanted into a rat had been verified to have generated the correct pattern of stimulation prior to implantation as explained above. Following explant of the stimulators after the five weeks of stimulation–denervation, oscilloscope measurements of the generated trains of bipolar pulses showed that the pulse amplitude, pulse width, and frequency were maintained as programmed.

This study utilized 32 rats. EDL muscles of 5 rats were denervated but not stimulated. Stimulators were implanted into the remaining 27 rats, of which data from 5 rats were excluded from the analysis because the stimulator failed to generate visible foot movement prior to final evaluation (3 rats), the waveform generated by the stimulator during the post-explant test was outside the specified parameters (1 rat), or the procedure to evaluate the muscle was not followed correctly (1 rat). Therefore, 15% (4 out of 27) of the stimulators became defective during the five week period of stimulation–denervation of this initial study.

4.2. Outcome for P_c (number of pulses per contraction)

Figs 10 and 11 show results from this study seeking values of P_c that maintain muscle mass and maximum force for five week stimulated–denervated EDL muscles of rats. Stimulators were programmed having P_c equal to 3, 6, or 20 pulses per contraction. The other stimulation variables were fixed (V_p=7 V, t_p=0.4 ms, F_p=100 Hz, C_d=100 contractions per day). A denervated group (P_c=0) of EDL muscles received no electrical stimulation. As seen in Fig. 10, increasing P_c up to 20 pulses per contraction progressively improved the retention of both muscle mass and maximum force. The data values were plotted as a percent of the control values of innervated, contralateral muscles. With P_c=0, the denervated EDL muscle retained only 35% of muscle mass and 10% of maximum force compared with innervated control muscles, but with P_c=20, the mass and maximum force were both more than 80% of control values.

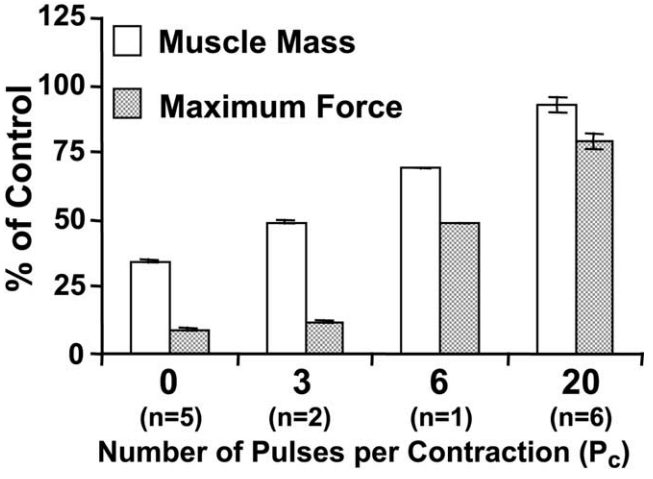

Fig. 10. Outcome for different numbers of pulses per contraction (P_c) for five week denervated EDL muscles of rats stimulated at V_p=7.0 V, C_d=100 contractions per day, F_p=100 Hz, t_p=0.4 ms. The mass and maximum force values shown are from evaluations of the muscles when removed from the animal after the 5 week duration of denervation–stimulation. The mass and maximum force of denervated–stimulated muscles with only P_c=3 were similar to unstimulated denervated muscles (P_c=0). With P_c increasing up to 20, the muscle mass and maximum force approached control values. Error bars are S.E.M.

The final number of muscles in each group was unbalanced because this series of experiments was intended to (1) demonstrate that the stimulator units would function adequately, and (2) to seek stimulation parameters that could maintain mass and force of stimulated–denervated muscles. When it became clear that certain stimulation values were ineffective, no further animals were used to increase the size of that group. Of the 2 rats implanted with stimulators for the P_c=6 group, data for one were excluded because the stimulator became defective and did not generate muscle contractions or foot movement prior to muscle evaluation. It is important to note that our method was to iteratively adjust the parameters to seek a combination of stimulation parameters that would maintain mass and force. We did not design this preliminary experiment to demonstrate statistically significant differences between groups.

In addition to the maintenance of muscle mass and maximum force, the structure of the muscle fibers was also better maintained with P_c=20 compared to lower P_c values. Fig 11(a) shows the cross-section of a contralateral control muscle. Fig. 11(b) shows a denervated muscle that received no electrical stimulation. The denervated fibers (P_c=0, Fig. 11(b)), have much smaller cross-sectional areas, more central nuclei, and a greater percentage of extracellular space in the tissue compared with control muscles (Fig. 11(a)). The stimulated–denervated fibers that received P_c=3 (Fig. 11(c)) appear much more similar to the unstimulated denervated fibers (Fig. 11(b)) than to the control fibers (Fig. 11(a)). The higher values of P_c=6 (Fig. 11(d)) or P_c=20 resulted in fiber structure similar to that of control muscles (Fig. 11(a)).

4.3. Outcome for V_p (pulse amplitude)

Figs 11 and 12 show results from the study seeking values of V_p that maintain muscle mass and maximum force for five week stimulated–denervated EDL muscles of rats. The amplitude of the pulses was varied while holding the other stimulation variables constant (t_p=0.4 ms, F_p=100 Hz, P_c=20, C_d=300). As seen in Fig. 12, higher levels of pulse amplitude, from 0 to 11 V, resulted in muscle mass and maximum force being maintained at values closer to control values. The stimulation protocols

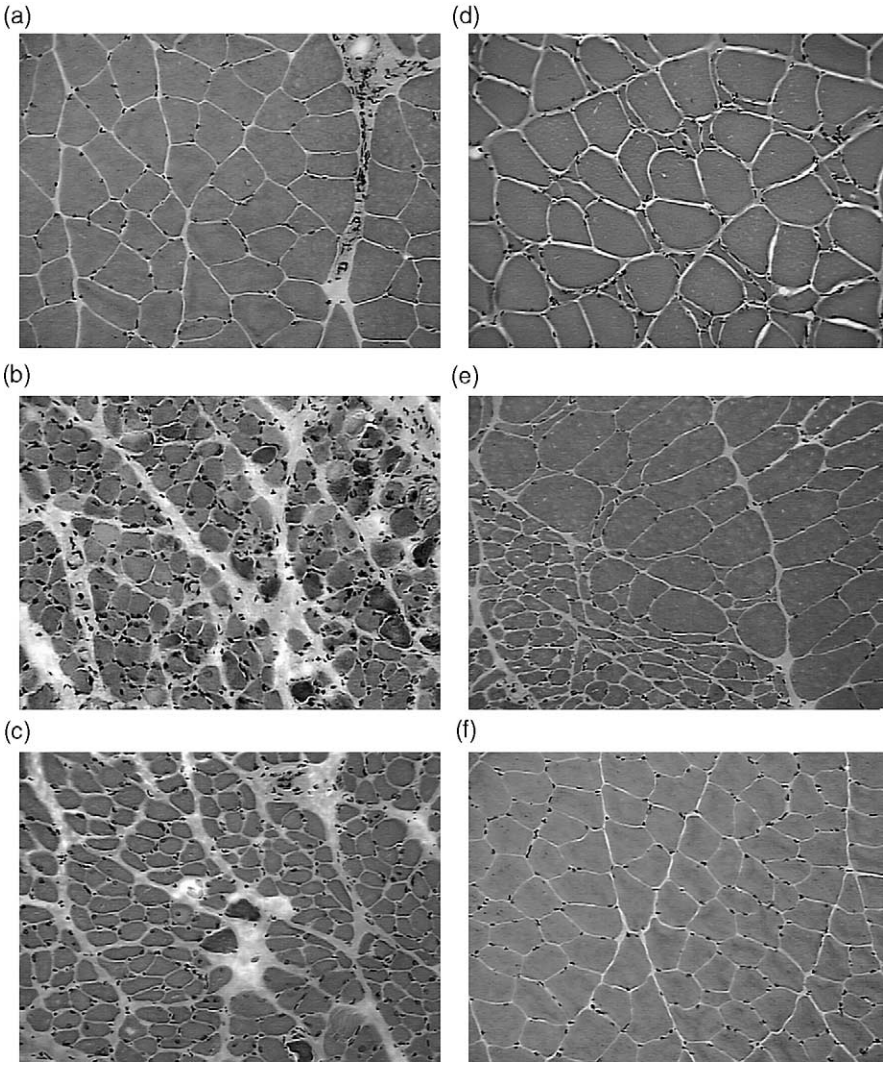

Fig. 11. Histological sections of EDL muscles of rats showing the effect of pulse voltage and number of pulses per contraction. (a) innervated control muscle; (b) denervated, unstimulated muscle; (c) 3 pulses per contraction, 7.0 V, 100 contractions per day; (d) 6 pulses per contraction, 7.0 V, 100 contractions per day; (e) 20 pulses per contraction, 5.0 V, 300 contractions per day; (f) 20 pulses per contraction, 9.0 V, 300 contractions per day. All electrically stimulated muscles received pulses at 100 Hz and having 0.4 ms pulse width. Sections were cut 10 μm thick and stained with hematoxylin and eosin (H&E) stain.

having either V_p=9 or 11 V maintained mass and maximum force approximately at the levels of control muscles.

The final number of muscles in each group was once again unbalanced for the same reasons explained above. Of the 3 rats implanted with stimulators for the V_p=9 volt group, data for one rat were excluded because the procedure to evaluate the muscle was not followed correctly. Of the 11 rats implanted with stimulators for this V_p=7 volt group, data for 4 were excluded from the final analysis since the stimulator did not generate foot movement (2 rats) or the waveform generated by the stimulator during the post explant test was incorrect (1 rat), or else the procedure to evaluate the muscle was not followed correctly (1 rat).

The structure of the muscle fibers was also better maintained in the muscles receiving higher pulse amplitudes. Fibers stimulated at V_p=5 V (Fig. 11(e)) were not maintained as well as fibers stimulated at V_p=9 V (Fig. 11(f)). Pulses having lower voltages seem to result in a higher population of small fibers that appear similar to fibers of denervated muscles (Fig. 11(b)). None of the stimulation protocols tested in this experiment resulted in apparent tissue damage visible in the light microscope H&E sections (data not shown).

5. Discussion: animal experiments

These studies verified that the described programmable, battery powered stimulator can generate muscle contractions in denervated EDL muscles of rats for five

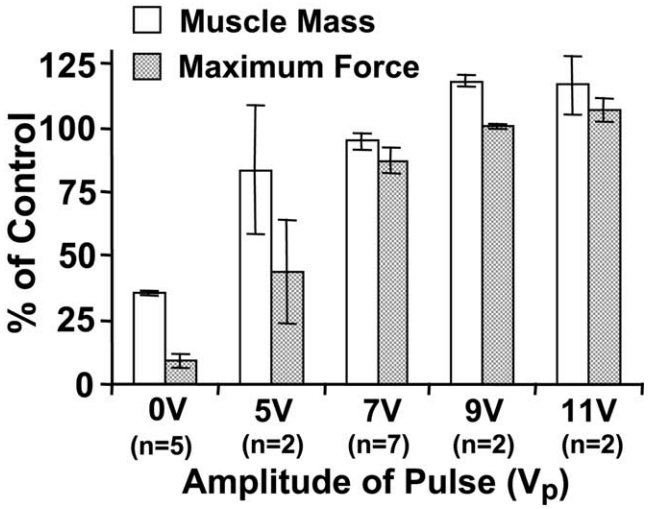

Fig. 12. Effect of pulse amplitude (V_p) for five week denervated EDL muscles of rats stimulated at P_c=20 pulses per contraction, C_d=300 contractions per day, F_p=100 Hz, t_p=0.4 ms. Chronic stimulation pulse amplitude ranged from 5 V to 11 V. The mass and maximum force values shown are from evaluations of the muscles when removed from the animal after the 5-week duration of denervation–stimulation. All denervated–stimulated muscles had higher muscle mass and maximum force than unstimulated denervated (V_p=0 V) muscles. Maximum force progressively increased as pulse amplitude increased from 5 V to 11 V. Error bars are S.E.M.

weeks, and the stimulator can be programmed to generate different protocols of stimulation that result in different values of muscle mass and maximum force. Of the stimulators implanted in rats during these studies, 85% continued to function correctly without failure for the full five week duration of the study.

Though the numbers of rats in the different groups of these initial studies are small and unbalanced, the results are promising and encourage further investigation. These data support our first hypothesis, that contractile activity generated by implantable electrical stimulators maintains muscle mass and maximum force at values similar to control values of innervated muscles. The data verify previous findings that electrical stimulation generates contractile activity in denervated muscles, thus reducing the progressive declines in the muscle properties that occur following the onset of denervation [1,3,6–8,19,41]. Not only did electrical stimulation reduce the declines, but certain protocols of stimulation in this study maintained muscle mass and maximum force at values similar to control values of innervated muscles.

The data also support the second hypothesis, that contractions sufficient to maintain muscle mass and maximum force are not generated if the number of pulses per contraction or the pulse amplitude is too low. Stimulation with only 3 pulses per contraction (F_p=100 Hz, C_d=100) did not maintain muscle mass and maximum force any better than a denervated muscle that received 0 pulses per contraction, but 20 pulses per contraction maintained muscle mass at 92±3% and maximum force at 79±4% of control values. In contrast to our results, Eken and Gundersen [6] found that a triplet pattern of 3 pulses per contraction (F_p=100–200 Hz, C_d=864) maintained the muscle mass and maximum force at values not different from a pattern of 25 pulses per contraction (F_p=150 Hz, C_d=96 or 5760). One difference was that our protocol separated each of the 3 pulses with 10 ms, whereas Eken and Gundersen separated the first two pulses with only 5 ms and separated the second and third pulses with 10 ms. A possible explanation of the differing results is that the force of tetanic contraction is lower when generated by 3 pulses spaced equally at 10 ms when compared to the uneven triplet pattern such as that employed by Eken and Gundersen. Further research will have to be done to resolve the different effects resulting from the different stimulation patterns having 3 pulses per contraction.

The data do support our hypothesis in that 6 and 20 pulses per contraction maintained mass and force better than 3 pulses per contraction, and the larger number of pulses generated larger foot movements during contractions. We visually observed that the 20 pulses per contraction protocol generated definite limb movement, the 6 pulses per contraction protocol generated smaller but visible limb movement, and the 3 pulses per contraction protocol generated very slight or no visible limb movement. In addition, a pulse amplitude of less than 3 V did not generate a measurable contraction during the preliminary acute study, and during this five week study a pulse amplitude of only 5 V maintained only 84% muscle mass and 44% maximum force, while pulse amplitudes of either 9 or 11 V maintained mass and force at nearly control values. Thus, either too few pulses per contraction or too low a pulse amplitude were shown to result in lower levels of maintained muscle mass and maximum force.

Furthermore, the stimulus amplitude that we identified as adequate for maintaining the mass and force at levels near control values may not have been sufficient to generate maximal tetanic contractions of the EDL muscles, as indicated by both the data plotted in Fig. 3 and prior results for which the EDL muscle of control rats consistently generated in excess of 2000 mN of force [30]. This counter intuitive result would indicate that full recruitment of all fibers within a denervated muscle may not be required for the maintenance of mass and contractility of denervated muscles. We conclude that muscle mass and maximum force of denervated muscles may be maintained by a protocol of submaximal electrically generated contractions. This may be due to a number of mechanisms, such as compensatory hypertrophy of some of the fibers that are recruited. Further studies will be necessary to elucidate the protective mechanisms involved.

Of the stimulation protocols tested, the protocol that best maintained muscle mass and maximum force gener-

ated 20 pulses per contraction and 100 contractions per day. This resulted in a total of only 2000 stimulus pulses per day. This value is somewhat less than the normal number of pulses seen in normally-innervated, freely moving adult rat EDL motor units, in which the number of pulses per day ranges from about 2,600 to about 243,000 [41]. It is possible that the optimal frequency of stimulation during each contraction is lower than 100 Hz, since Hennig and Lomo also found that muscles tend to operate in the middle of the sigmoidal frequency–force range to permit the best modulation of muscle force, which for adult rat EDL muscles is about 40 to about 90 Hz [41]. This supports the idea that the optimal number of stimulus pulses for stimulated–denervated muscles is equivalent to the number of pulses per day in normally innervated control muscles, even though our protocol was at the lower end of this range.

6. Conclusions

We designed a battery powered, pre-programmable stimulator and verified its function by implanting stimulators into rats. Denervated EDL muscles of rats were electrically stimulated for five weeks and evaluated in terms of muscle mass and maximum force. Stimulation protocols of 9–11 V pulse amplitude, 0.4 ms bipolar pulse width, 100 Hz frequency of pulses, 20 pulses per contraction, and 100 or 300 contractions generated per day maintained muscle mass and maximum force at levels near to control values for innervated muscles. There is more work to be done to optimize the stimulation protocol for particular muscles and applications. Rather than optimizing the protocol in terms of muscle mass and maximum force, a study or application may require optimization for the maintenance of tissue excitability, extracellular matrix composition, tissue architecture, or specific gene expression. The described implantable stimulator is economical and readily assembled by many laboratories. This enables further experimentation of stimulation–denervation in freely moving animals housed in regular animal facilities. The ability to be preprogrammed enables customized, complex protocols of stimulation for optimization and tissue response studies.

Acknowledgements

The authors would like to thank Cheryl Hassett for her important contributions to the development of techniques for surgical implantation of the stimulators and electrodes, and for subsequent removal of the muscles for evaluation. This work was supported by grants NIH #2 PO1 AG 10821, and NIA #AG00114-17.

References

[1] Reid J. On the relation between muscular contractility and the nervous system. London Edinburgh Monthly J Medical 1841;1:320–9.
[2] Eberstein A, Eberstein S. Electrical stimulation of denervated muscle: is it worthwhile? Medicine and Science in Sports and Exercise 1996;28(12):1463–9.
[3] Osborne SL. The retardation of atrophy in man by electrical stimulation in muscles. Archives of Physical Medicine 1951;32:523–8.
[4] Elliott DR, Thomson JD. Dynamic properties of denervated rat muscle treated with electrotherapy. American Journal of Physiology 1963;205(1):173–6.
[5] Al-Amood WS, Finol HJ, Lewis DM. Chronic stimulation modifies the isotonic shortening velocity of denervated rat slow-twitch muscle. Proc R Soc Lond B 1986;228:43–58.
[6] Eken T, Gundersen K. Electrical stimulation resembling normal motor-unit activity: effects on denervated fast and slow rat muscles. Journal of Physiology 1988;402:651–69.
[7] Gundersen K, Eken T. The importance of frequency and amount of electrical stimulation for contractile properties of denervated rat muscles. Acta Physiol Scand 1992;145:49–57.
[8] Lomo T, Westgaard RH, Engebretsen L. Different stimulation patterns affect contractile properties of denervated rat soleus muscles. In: Pette D, editor. Plasticity of muscle. Berlin: De Gruyter; 1980, p. 297–309.
[9] Williams HB. The value of continuous electrical muscle stimulation using a completely implantable system in the preservation of muscle function following motor nerve injury and repair: an experimental study. Microsurgery 1996;17:589–96.
[10] Nicolaidis SC, Williams HB. Muscle preservation using an implantable electrical system after nerve injury and repair. Microsurgery 2001;21:241–7.
[11] Kern H, Hofer C, Modlin M, Forstner C, Raschka-Hogler D, Mayr W, Stohr H. Denervated muscles in humans: limitations and problems of currently used functional electrical stimulation training protocols. Artif Organs 2002;26(3):216–8.
[12] Kern H, Hofer C, Strohhofer M, Mayr W, Richter W, Stohr H. Standing up with denervated muscles in humans using functional electrical stimulation. Artif Organs 1999;23(5):447–52.
[13] Hofer C, Mayr W, Stohr H, Unger E, Kern H. A stimulator for functional activation of denervated muscles. Artificial Organs 2002;26(3):276–9.
[14] Jarvis JC, Salmons S. A family of neuromuscular stimulators with optical transcutaneous control. Journal of Medical Engineering & Technology 1991;15(2):53–7.
[15] Dennis RG. Bipolar implantable stimulation for long-term denervated-muscle experiments. Medical & Biological Engineering & Computing 1998;36:225–8.
[16] Dennis RG, Kosnik P. Excitability and isometric contractile properties of mammalian skeletal muscle constructs engineered in vitro. In Vitro Cell Dev Biol Anim 2000;36(5):327–35.
[17] Dennis RG, Kosnik PE, Gilbert ME, Faulkner JA. Excitability and contractility of skeletal muscle engineered from primary cultures and cell lines. Am J Physiol Cell Physiol 2001;280(2):C288–C95.
[18] Kosnik PE, Faulkner JA, Dennis RG. Functional development of engineered skeletal muscle from adult and neonatal rats. Tissue Eng 2001;7(5):573–84.
[19] Liu ET, Lewey FH. The effect of surging currents of low frequency in man on atrophy of denervated muscles. The Journal of Nervous and Mental Disease 1947;105:571–81.
[20] Pachter BR, Eberstein A, Goodgold J. Electrical stimulation effect on denervated skeletal myofibers in rats: a light and electron microscopic study. Arch Phys Med Rehabil 1982;63:427–30.
[21] Chang CW, Lien IN. Tardy effect of neurogenic muscular atro-

phy by magnetic stimulation. American Journal of Physical Medicine & Rehabilitation 1994;73(4):275–9.
[22] Gorza L, Gundersen K, Lomo T, Schiaffino S, Westgaard RH. Slow-to-fast transformation of denervated soleus muscles by chronic high-frequency stimulation in the rat. Journal of Physiology 1988;402:627–49.
[23] Lewis DM, Al-Amood WS, Schmalbuch H. Effects of long-term phasic electrical stimulation on denervated soleus muscle: guinea-pig contracted with rat. Journal of Muscle Research and Cell Motility 1997;18:573–86.
[24] Ziaie B, Nardin MD, Coghlan AR. A single-channel implantable microstimulator for functional neuromuscular stimulation. IEEE Transactions on Biomedical Engineering 1997;44(10):909–20.
[25] Loeb GE, Peck RA, Moore WH, Hood K. BION system for distributed neural prosthetic interfaces. Medical Engineering & Physics 2001;23(1):9–18.
[26] Bhadra N, Kilgore KL, Peckham PH. Implanted stimulators for restoration of function in spinal cord injury. Medical Engineering & Physics 2001;23(1):19–28.
[27] Jarvis JC, Salmons S. The application and technology of implantable neuromuscular stimulators: an introduction and overview. Medical Engineering & Physics 2001;23(1):3–7.
[28] Salmons S, Gunning GT, Taylor I, Grainger SRW, Hitchings DJ, Blackhurst J, Jarvis JC. ASIC or PIC? Implantable stimulators based on semi-custom CMOS technology or low-power microcontroller architecture. Medical Engineering & Physics 2001;23(1):37–43.
[29] Ausoni S, Gorza L, Schiaffino S, Gundersen K, Lomo T. Expression of myosin heavy chain isoforms in stimulated fast and slow rat muscles. The Journal of Neuroscience 1990;10(1):153–60.
[30] Carlson BM, Billington L, Faulkner J. Studies on the regenerative recovery of long-term denervated muscle in rats. Restorative Neurology and Neuroscience 1996;10:77–84.
[31] Lu DX, Huang SK, Carlson BM. Electron microscopic study of long-term denervated rat skeletal muscle. The Anatomical Record 1997;248:355–65.
[32] Viguie CA, Lu DX, Huang SK, Rengen H, Carlson BM. Quantitative study of the effects of long-term denervation on the extensor digitorum longus muscle of the rat. The Anatomical Record 1997;248:346–54.
[33] Lomo T. Long-term effects of altered activity on skeletal muscle. Biomedica Biochimica Acta 1989;48(5–6):S432–S44.
[34] Dennis RG, Dow DE, Hsueh A, Faulkner JA. Excitability of engineered muscle constructs, denervated and denervated–stimulated muscles of rats, and control skeletal muscles in neonatal, young, adult, and old mice and rats. Biophysical Journal 2002;82(1):364A.
[35] Carlson BM, Faulkner JA. Reinnervation of long-term denervated rat muscle freely grafted into an innervated limb. Experimental Neurology 1988;102:50–6.
[36] Miller SW, Dennis RG. A parametric model of muscle moment arm as a function of joint angle: application to the dorsiflexor muscle group in mice. J Biomechanics 1996;29(12):1621–4.
[37] Lilly JC. Injury and excitation by electric currents. A. The balanced pulse-pair waveform. In: Sheer DE, editor. Electrical stimulation of the brain. TX: University of Texas Press; 1961.
[38] Donaldson NDN, Donaldson PEK. When are actively balanced biphasic ('Lilly') stimulating pulses necessary in a neurological prosthesis? Medical & Biological Engineering & Computing 1986;24:50–6.
[39] Scheiner A, Mortimer JT, Roessmann U. Imbalanced biphasic electrical-stimulation-muscle-tissue damage. Annals of Biomedical Engineering 1990;18(4):407–25.
[40] Faulkner JA, Brooks SV, Dennis RG. Measurement of recovery of function following whole muscle transfer, myoblast transfer, and gene therapy. In: Morgan JR, Yarmush ML, editors. Tissue engineering methods and protocols. Totowa, NJ: Humana Press; 1999, p. 155–172.
[41] Hennig R, Lomo T. Firing patterns of motor units in normal rats. Nature 1985;314:164–6.